Proceedings of ICRC 2001: 3005 © Copernicus Gesellschaft 2001

ICRC 2001

The flux and spectrum of solar neutrinos at Super-Kamiokande

E. Blaufuss for the Super-Kamiokande Collaboration

Department of Physics, University of Maryland, College Park, MD, USA

Abstract. Data collected at the Super-Kamiokande detector have been used to make observations of the flux and spectrum of neutrinos that originate in the fusion reactions inside the center of the Sun. Solar neutrinos are observed at Super-Kamiokande through the detection of the recoil electron from neutrino-electron scattering in the water of the detector. The measured flux is 2.32±0.03(stat.) ±0.08(syst.)×10^6/cm^2/s, which is 0.451 the flux predicted by the latest Bahcall and Pinsonneault solar model. Observations of the spectrum of recoil electrons above 5.0 MeV and variations in the neutrino flux in different times of the day and different seasons of the year are also performed. The implications of these results for the solution to the solar neutrino problem by neutrino oscillations are also discussed.

1 Introduction

Energy is produced in the Sun through nuclear fusion. For a star such as the Sun, this involves turning 4 protons into a helium nucleus to tap the α particle binding energy. For every α particle made, two neutrinos are produced. The neutrinos, due to their small interaction cross section, escape the Sun, essentially undergoing no interactions.

Solar neutrinos have been previously detected in chlorine-, gallium-, and water-based detectors (B.T. Cleveland et al. (1998); J.N. Abdurashitov et al. (1999); P. Anselmann et al. (1994); Y. Fukuda et al. (1996)). These experiments were each sensitive to different neutrino energy ranges, but all found fluxes significantly lower than those predicted by complex models of the solar interior, known as Standard Solar Models (SSMs; J.N. Bahcall et al. (2000, 1998)). This discrepancy between the predicted and measured flux of solar neutrinos is known as "*the solar neutrino problem.*" The solution to the solar neutrino problem is generally believed to involve neutrino oscillations.

Recent evidence (Y. Fukuda et al. (1998)) indicates that at least some flavors of neutrinos are massive. Neutrino mass naturally leads to interesting effects like oscillation of neutrino flavor, where neutrinos change from one flavor state to another as they propagate through space. Two component neutrino oscillations are typically parameterized by the difference of the squared masses between the two eigenstates (Δm^2) and the mixing angle ($\sin^2 2\theta$). The survival probability of an electron neutrino state of energy E remaining an electron neutrino after traveling a distance L is given by:

$$P(\nu_e \to \nu_e; L) = 1 - \sin^2 2\theta \sin^2 \left[1.27 \frac{\Delta m^2[\text{eV}^2] L[\text{m}]}{E[\text{MeV}]}\right] \quad (1)$$

The Super-Kamiokande (SK) detector was built to search for, among other things, the interaction of solar neutrinos. Neutrinos of sufficient energy ($\gtrsim$6 MeV) are detected in real-time by the elastic scatter of electrons. These scattered electrons are used to measure the flux of solar neutrinos, as well as searching for any possible distortions in the neutrino spectrum, and any short or long term time dependence of the flux. An observation of a measurable day/night flux difference, a distortion of the neutrino energy spectrum, or a seasonal dependence to the neutrino flux would provide strong solar model independent evidence of neutrino oscillations.

2 Super-Kamiokande Detector

SK is a water Cherenkov detector located in the Kamioka Mine in Gifu, Japan. The cylindrical detector is divided into an inner and outer detector (ID and OD, respectively) by a stainless-steel frame structure that serves as an optical barrier and a mounting point for all photo-multiplier tubes (PMTs). Cherenkov light in the ID is collected by 11,146 inward facing $50\,cm$ PMTs mounted uniformly on the wall, providing 40% photo-cathode coverage. In the OD, 1885 outward facing $20\,cm$ PMTs monitor the $2.5\,m$ thick veto region. The veto tags incoming particles and is a passive shield for gamma activity from the surrounding rock. The fiducial volume for the analysis of neutrino events starts $2\,m$ inward of the walls of the ID and contains $22.5\,kton$ of pure water.

Recoil electrons from solar neutrinos seen in SK have energies that range from 5 to 18 MeV. At these energies, the electron is limited to a few centimeters in range and the vertex position is found using the relative timing of hit PMTs,

Correspondence to: E.Blaufuss
(blaufuss@umdgrb.umd.edu)

assuming that all Cherenkov photons came from a single point. Once a vertex is reconstructed, the direction of the electron is determined using the characteristic shape of the emitted Cherenkov radiation. The energy of the scattered electron is determined from the number of hit PMTs.

In order to set the absolute energy scale of the detector, a linear accelerator of electrons (LINAC) has been installed at the detector (M. Nakahata et al. (1999)). This system allows electrons of a known, fixed energy to be injected into the detector. The energy scale has also been cross checked with the well-known β decay of ^{16}N, which is produced *in situ* by an (n,p) reaction on ^{16}O. The fast neutrons needed for this reaction are produced by a portable deuterium-tritium neutron generator (DTG; E. Blaufuss et al. (2001)). The energy scale measured with the DTG agrees with the LINAC to within $\pm 0.3\%$. The total uncertainty in the absolute energy scale is $\pm 0.6\%$.

The results in this paper are derived from data taken between May 31, 1996 and October 6, 2000, representing 1258 live days. The raw data sample consists of 2.0×10^9 triggered events before any background reduction is performed. This sample is reduced through a series of cuts designed to remove known sources of background, including high energy cosmic ray muons and their spallation products, events generated by electrical noise and arcing in the PMTs, and external gamma-ray activity. Additional cuts are performed to remove likely background events with poorly defined vertex positions (S. Fukuda et al. (2001)). After the reduction, a sample of 236,140 events remain, with a signal-to-noise ratio of $\sim$1 in the direction of the Sun.

The neutrino and scattered electron have a strong angular correlation, and the solar neutrino signal is extracted from the data using the $\cos\theta_{sun}$ distribution. The value of θ_{sun} is the size of the angle between the recoil electron momentum and a vector connecting the Sun to the Earth. The distribution of $\cos\theta_{sun}$ for the reduced data sample is shown in Figure 1. A strong peak from solar neutrino events is seen. The number of solar neutrino events is extracted from the $\cos\theta_{sun}$ distribution using a likelihood function that fits the measured background shape and the expected signal shape, based on a detector simulation of solar neutrino events, to the data. This fit is also shown in Figure 1 as a solid line. After 1258 days, a total of $18,464 \pm 204$(stat.)$^{+646}_{-554}$(sys.) signal events are found.

3 Measured Results

The number of signal events is translated into a measured flux using a full detector Monte Carlo simulation taking the input flux and spectrum from the reference SSM, and comparing this to the number of measured signal events. Our detector simulation is based on GEANT 3.21 (GEANT (1994)). Neutrinos that produce recoil electrons with energies > 5MeV are produced almost entirely from the β decay of ^{8}B in the solar interior, with a slight admixture of neutrinos from the ^{3}He-p (hep) fusion reaction. The flux normalization for both

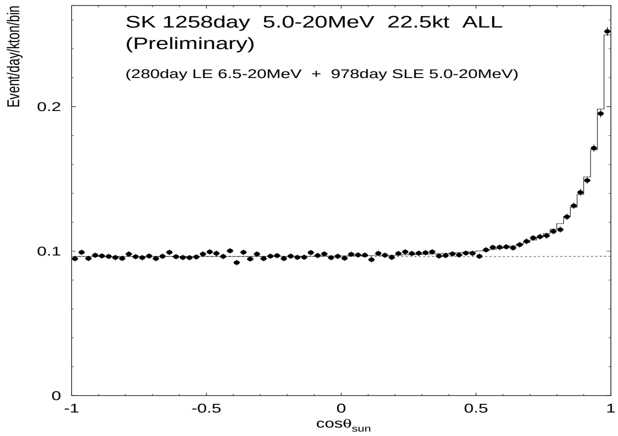

Fig. 1. The $\cos\theta_{sun}$ distribution for events in the reduced sample of solar neutrino candidates. The best fit to signal+background is shown as the solid line, while the measured background shape is shown as a dashed line.

fluxes and spectral shape for hep are taken from the BP2000 SSM (J.N. Bahcall et al. (2000)). For the ^{8}B neutrino spectral shape, we have taken the recent improved measurement of Ortiz et al. (C.E. Ortiz et al. (2000))

The number of signal events obtained from the $\cos\theta_{sun}$ distribution represents 45.1$\pm$0.5(stat.)$^{+1.6}_{-1.4}\%$ of the reference flux. The corresponding ^{8}B flux at 1 AU is:

$$2.32 \pm 0.03(\text{stat.})^{+0.08}_{-0.07}(\text{sys.}) \times 10^6 cm^{-2}s^{-1}. \quad (2)$$

The solar neutrino flux as a function of zenith angle is also measured, and the results shown in Figure 2. The zenith angle (θ_z) is defined as the angle between the vertical axis at the SK detector and the vector connecting the Sun to the Earth. The night-time solar neutrino flux is measured when $\cos\theta_z > 0$, while the day-time flux is measured when $\cos\theta_z < 0$. Additionally, to search for enhancement in the flux for neutrinos passing through the core of the Earth, the night-time period is divided into 6 zenith bins. The flux measured in each of the these zenith bins, relative to the expectations from the reference SSM, are shown in Figure 2. The flux asymmetry between night- and day-time total fluxes is found to be:

$$\frac{\Phi_n - \Phi_d}{\frac{1}{2}(\Phi_n + \Phi_d)} = 0.033 \pm 0.022(\text{stat.})^{+0.013}_{-0.012}(\text{sys.}) \quad (3)$$

The flux as a function of season is shown in Figure 3, along with the expected variation from the Earth's eccentricity. The measured data are consistent (χ^2/d.o.f. $= 3.9/7$) with the expected annual seasonal variation. A fit to a flat distribution has a χ^2/d.o.f. $= 8.1/7$.

In order to search for distortions in the neutrino energy spectrum, the recoil electron spectrum is examined. This spectrum is obtained by repeating the flux measurement for small slices in recoil electron energy. The measured recoil electron spectra is steeply falling, and is therefore normalized to the expectations from the reference SSM. The normalized

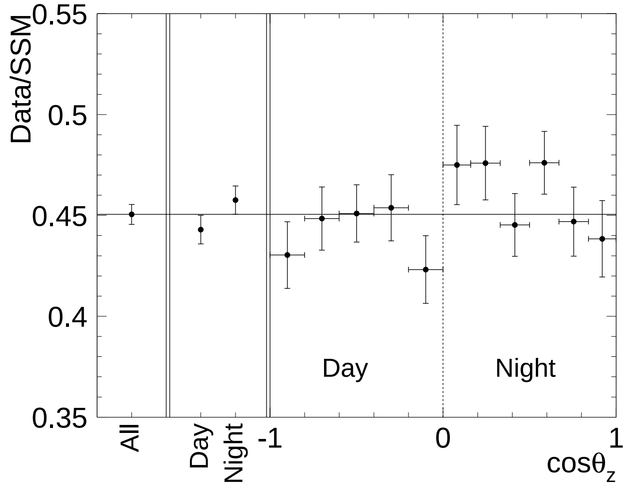

Fig. 2. Measured solar neutrino flux as a function of zenith angle, relative to the reference SSM flux. The horizontal line represents the flux measured for all data. The extreme right bin represents data collected after passing through the Earth's core ($\cos\theta_z > 0.84$).

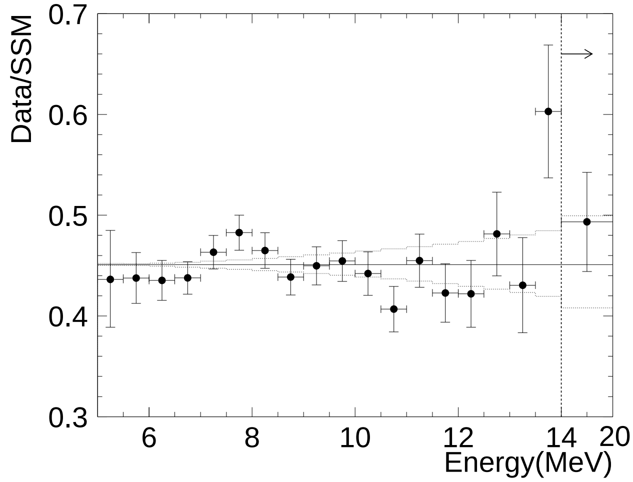

Fig. 4. The measured recoil electron spectrum measured at SK, normalized to the expectations from the reference SSM. Also shown are the energy correlated systematic errors (dotted band) that arise from the uncertainties in the energy scale, the energy resolution and the reference ^{8}B spectrum.

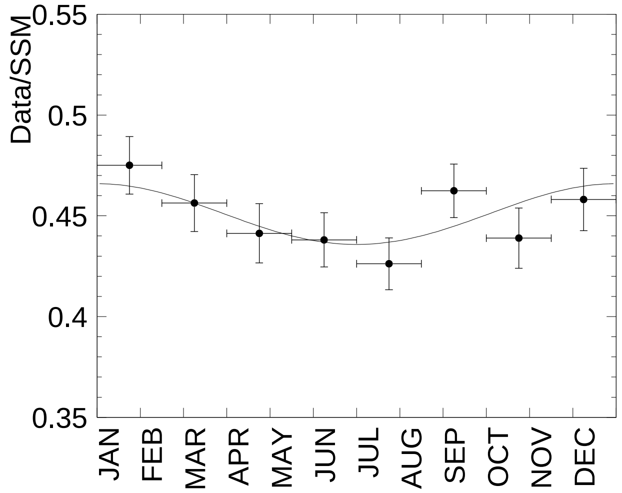

Fig. 3. The seasonal dependence of the solar neutrino flux, relative to the reference SSM. The solid line shows the expected shape and shape of the variation in solar neutrino flux due to the Earth's eccentricity.

recoil electron spectrum is shown in Figure 4. A fit to an undistorted spectrum (flat) gives a $\chi^2/\text{d.o.f.} = 19.1/18$. Figure 4 also presents the energy correlated systematic errors that arise from the uncertainties in the energy scale, the energy resolution and the reference ^{8}B spectral shape. These are the errors that could cause a systematic shift in the measured recoil electron spectral shape, and these errors are considered in the definition of the χ^2(Y. Fukuda et al. (1999)).

3.1 Oscillation Analysis

As the measured results show no significant deviation from the expectations of the reference SSM, no solar model independent evidence of neutrino oscillations is observed. Therefore, the measured results are used to generate exclusion regions in the neutrino oscillation parameter space where strong deviations are predicted. The measured flux, in combination with the measured recoil electron spectral shape and zenith angle dependence are also used to find allowed regions in this space, areas where the predicted spectral shape, zenith angle dependence and flux are consistent with the observed values.

For this analysis, the data were divided into seven zenith angle bins (one day bin, 6 bins in $\cos\theta_z$ at night). These zenith angle bins are further divided into eight recoil electron energy bins, to create a "zenith angle energy spectrum" (S. Fukuda et al. (2001)). For each set of neutrino oscillation parameters ($\sin^2 2\theta$ and Δm^2), the expected number of solar neutrinos and the corresponding zenith angle energy spectrum are calculated using a numerical calculation of neutrino survival probabilities, taking into account matter effects as the neutrino propagates from the center of the Sun to the SK detector here on the Earth. The measured and expected zenith angle energy spectrum are compared using a χ^2 analysis at each set of neutrino oscillation parameters. This analysis was performed under a two component neutrino oscillation hypothesis, once for active neutrinos ($\nu_e \rightarrow \nu_{\mu,\tau}$) and once for sterile neutrinos ($\nu_e \rightarrow \nu_{\text{sterile}}$).

The results of this analysis are shown in Figure 5 for the active case and in Figure 6 for the sterile case. The large, red shaded regions in these figures represent the 95% confidence level (C.L.) exclusion regions based on a flux-independent analysis of the zenith angle energy spectrum. Additionally, the measured zenith angle energy spectrum measured, the measured flux, and the theoretical uncertainty of ^{8}B neutrino flux are used to generate allowed regions at the 95% C.L. These are regions that are consistent with the observed zenith angle energy spectrum and flux measured at SK and are shown in the figures as the thin, blue shaded regions near

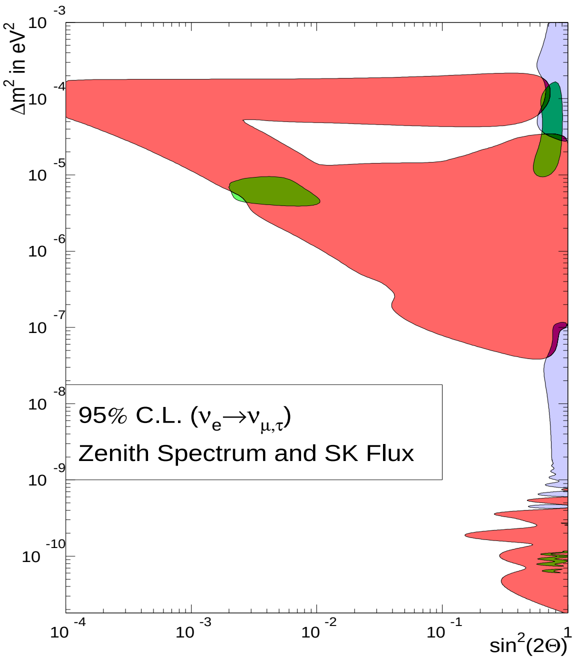

Fig. 5. Neutrino oscillation excluded/allowed regions for the case of active neutrinos. Red shaded regions represent the 95% C.L. exclusion regions based on a flux-independent zenith angle energy spectrum analysis. The blue shaded regions represent the 95% C.L. allowed regions for an analysis of the zenith angle energy spectrum with a flux constraint for SK data based on the reference SSM. The green shaded regions are the allowed regions at the 95% C.L. based on a flux-only analysis based on the results from SK, in combination with the results from the gallium and chlorine experiments.

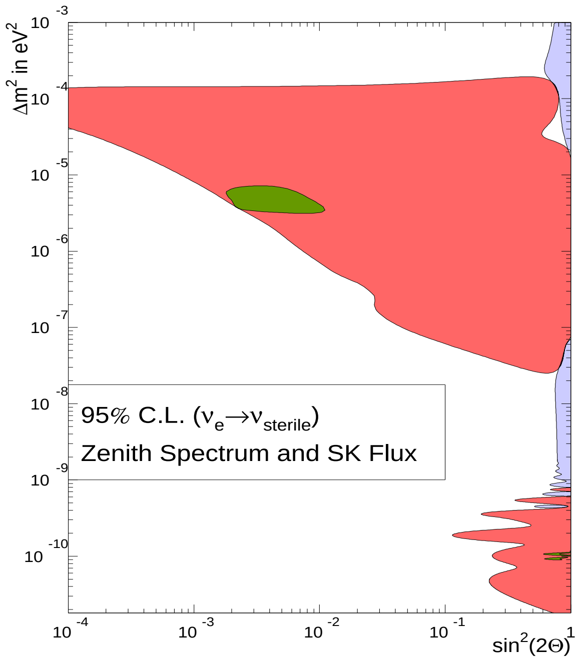

Fig. 6. Neutrino oscillation excluded/allowed regions for the case of sterile neutrinos. Region definitions are the same as Figure 5.

maximal mixing. Finally, the flux measured at SK is combined with the total fluxes measured in the gallium and chlorine experiments to generate flux-only allowed regions at the 95% C.L. These are regions that predict the correct oscillated fluxes in all three types of solar neutrino experiments under the reference SSM inputs and are shown as green shaded regions in the figures.

The flux-only allowed regions must be consistent with the flux-independent zenith angle energy spectrum measured by SK to be considered as a valid solution. The overlap of a particular combined flux-only allowed region (green) with the exclusion regions from the zenith angle energy spectrum analysis (red) would be strong evidence against that allowed region. Because of this, all but a portion of one flux-only allowed region (green) for active neutrinos are excluded at the $> 90\%$ C.L. The current SK data favor the so called "Large Mixing Angle" solution ($\Delta m^2 \simeq 10^{-4} \sim 10^{-5}, \sin^2 2\theta > 0.5$) for active neutrinos. The lower portion of this flux-only allowed region is excluded from a lack of a strong day-night flux asymmetry, but the upper half is consistent with the zenith angle energy spectrum and flux measured at SK. All flux-only allowed regions for sterile neutrinos are disfavored at the 95% C.L.

In summary, the SK detector has precisely measured the flux, recoil electron spectrum, and time variation in the flux of ^{8}B solar neutrinos over a 1258 day period. These data show no strong model-independent evidence of neutrino oscillation and are therefore used to generate exclusion regions in the neutrino oscillation parameter space. The current data favor the Large Mixing Angle solution for active neutrinos.

Acknowledgements. We gratefully acknowledge the cooperation of the Kamioka Mining and Smelting Company. This work was partly supported by the Japanese Ministry of Education, Science and Culture, the U.S. Department of Energy and the U.S. National Science Foundation.

References

B.T. Cleveland et al., Astrophys. J. **496**, 505 (1998).
J.N. Abdurashitov et al., Phys. Rev. C **60**, 055801 (1999).
P. Anselmann et al., Phys. Lett. B **327**, 377 (1994).
Y. Fukuda et al., Phys. Rev. Lett. **77**, 1683 (1996).
J.N. Bahcall et al., astro-ph/0010346.
J.N. Bahcall et al., Phys. Lett. B **433**, 1 (1998).
Y. Fukuda et al., Phys. Rev. Lett **81**, 1562 (1998).
M. Nakahata et al., Nucl. Instr. Meth. A **421**, 113 (1999).
E. Blaufuss et al., Nucl. Instr. Meth. A **458**, 636 (2001).
S. Fukuda et al., hep-ex/0103032 (2001).
GEANT Detector Description and Simulation Tool, *Cern Programming Library W5013* (1994).
C.E. Ortiz et al., Phys. Rev. Lett. **85**, 2909 (2000).
Y. Fukuda et al., Phys. Rev. Lett. **82**, 2430 (1999).
S. Fukuda et al., hep-ex/0103033 (2001).